BMC Cancer

RESEARCH

Open Access

Diagnostic value of high-frame-rate contrast-enhanced ultrasound and contrast vector imaging for superficial lymph node lesions

Ruiying Li[1†], Xiaofeng Lan[1†], Xiang Xie[1*], Jun Wu[1], Rui Hu[1] and Jiale Guo[2]

Abstract

Purpose To explore the diagnostic performance and feasibility of high-frame-rate contrast-enhanced ultrasound (HFR CEUS) combined with contrast vector imaging (CVI) in detecting benign and malignant superficial lymph nodes (SLNs).

Materials and methods In this single-center prospective study conducted between October 2023 and February 2024, 38 consecutive patients with suspected SLN lesions underwent B-mode US, HFR CEUS examination, and post-processing CVI analysis. Their diagnosis was confirmed using fine-needle aspiration cytologic or histopathologic examination. The diagnostic efficacy of HFR CEUS alone and the combination of HFR CEUS with CVI for benign and malignant LN diagnosis was compared and the significance of other CVI parameters was evaluated.

Results The final data set included 38 participants (mean age, 56 ± 16 years) with 42 SLN lesions. Both HFR CEUS alone and HFR CEUS combined with CVI examination showed differences in the contrast patterns of benign and malignant SLNs (all $P < 0.001$). The contrast pattern of benign LNs was predominantly centrifugal, while that of malignant LNs was primarily centripetal and hybrid and they were more likely to exhibit perfusion defects. The comparison between CVI combined with HFR CEUS examination and pathological results for the diagnosis of benign and malignant LNs showed a high level of consistency with a kappa value of 0.81. Comparison with HFR CEUS alone resulted in a kappa value of 0.66.

Conclusion HFR CEUS combined with CVI examination demonstrated a good performance in distinguishing benign and malignant SLNs.

Keywords Superficial lymph node, High-frame-rate contrast-enhanced ultrasound, Contrast vector imaging

[†]Ruiying Li and Xiaofeng Lan contributed equally to this work.

*Correspondence:
Xiang Xie
sonographer@126.com
[1]Department of Ultrasound Medicine, The Second Affiliated Hospital of Anhui Medical University, Hefei City 230000, Anhui Province, China
[2]Anhui Medical University, Hefei City 230000, Anhui Province, China

Introduction

Superficial lymph node (SLN) lesions are complex and diverse. Most SLN lesion patients display no obvious clinical symptoms at the early stages, and sometimes LN enlargement is the only initial complaint. Theoretically, various diseases may contribute to LN enlargement, including cancer, infection, and tuberculosis [1]. At the same time, the incidence and mortality rates of malignant LN lesions have shown an upward trend in recent years [2]. Therefore, it is very important to clarify the nature of benign or malignant SLNs as early as possible for patient survival and optimal prognosis.

There are many imaging methods for the diagnosis of lymphadenopathy, including ultrasound (US), computed tomography (CT), magnetic resonance imaging, and positron emission tomography-CT [3, 4]. Among them, US is a commonly used imaging method as it can determine many important LN parameters and is more convenient and cost-effective compared to other examinations [5]. However, it is difficult to distinguish complex SLN lesions solely based on B-mode US [6]. Contrast-enhanced US (CEUS) combined with the use of US contrast agents can show the microvascular state and blood supply of LNs in real time [7]. High-frame-rate CEUS (HFR CEUS) enhances the temporal resolution of images by increasing the acquisition frame rate, thereby obtaining more detailed information about arterial phase perfusion [8–11]. However, CEUS results are subjective compared to those of other imaging examinations and there is currently no unified diagnostic standard. Accurate assessment of SLN lesions' angiographic patterns remains challenging. The emergence of post-processing contrast vector imaging (CVI) technology can effectively compensate for CEUS' shortcomings. CVI is a post-processing technique that can automatically match frames and track contrast bubbles, displaying the results in various forms by analyzing HFR US contrast images. It can quantitatively and objectively assess blood flow at the target site, while also obtaining additional qualitative information. Therefore, the combination of HFR CEUS with CVI technology can display the angiographic characteristics of the lesion with higher temporal and spatial resolution [12]. Many studies have reported on the effectiveness of HFR CEUS examination in the diagnosis of benign and malignant SLN lesions. However, there is no relevant research discussing the value of CVI technology in SLN lesions. Therefore, the present study aimed to explore the diagnostic value and feasibility of HFR CEUS combined with CVI in SLN lesions.

Materials and methods

Participants

The present prospective single-center cohort study was approved by the medical ethics committee (YX2023-211). All participants provided written informed consent before the examination. Consecutive participants with suspected SLN lesions who underwent conventional B-mode US and HFR CEUS examinations between October 2023 and February 2024 were subjected to fine-needle aspiration biopsy or histopathological examination of the target LN.

The inclusion criteria: those patients had suspicious lymph nodes that could not be determined as benign or malignant by two-dimensional ultrasound.

The following patients were excluded: (a) those who were allergic to contrast agents, (b) those who were pregnant, (c) those who had a history of surgery or radiation therapy, and (d) those who had undergone thermal ablation therapy.

Equipment and materials

The study experiments were carried out on an US system Aplio i900 (Canon Medical Systems, Tokyo, Japan) equipped with PLI-1205BX and PLI-705BX probes, in which the PLI-1205BX probe was used for B-mode US examination and the PLI-705BX probe was used for HFR CEUS examination. CEUS images were obtained in contrast-specific US mode (advanced pulse subtraction mode, HFR CEUS) with the following parameters: contrast harmonic frequency, 3.5–11.5 MHz; mechanical index, 0.12; dynamic range, 60 dB; gain, 75 dB; and frame rate, 49–51 frame/sec. With the HFR CEUS technique using multi-beam receiver and multi-harmonic compounding technique, high temporal resolution arterial phase imaging at 49–51 frames/sec was obtained and used for detecting bubble contrast agents and tracing bubble movements within the lesions. The contrast agent Sono Vue (Bracco Imaging S.p.A., Milan, Italy) was prepared by mixing the dry powder with 5 mL of normal saline.

Conventional B-mode US examination

Participants were scanned in a supine position, with their SLN lesions fully exposed. US examination was used to assess the size and vascular index (VI) in superb microvascular imaging and power Doppler of SLN lesions.

HFR CEUS combined with CVI examination

The relevant parameters were adjusted in the HFR CEUS mode. First, the patient was instructed to breathe calmly, and a nurse administered 2.5 mL of Sono Vue through the antecubital vein, followed by 5 mL of normal saline. The radiologist immediately recorded and stored the continuous HFR contrast images of the target lesion lasting for 60 s at the workstation. Post-processing online software, such as CVI, was equipped at the same US system (Aplio i900) used for HFR CEUS examination for convenience. The CVI software traced and automatically

matched the speckle pattern of each template image between frames [12]. There were seven display types: arrival time, direction, direction center, velocity, velocity variance, trace, and arrow. The trace and arrow visualized all of the detected bubbles, while the other five revealed their contiguous movement. Therefore, if a contrast bubble was detected on a certain frame and did not move or disappear in the following frame, it could not be visualized via the latter five display types. Furthermore, each display type was color-coded to provide information for the detected bubbles or regarding their movement in the form of either velocity or direction.

Pathological examination

A fine-needle aspiration biopsy or a histopathologic examination was performed on the LNs after B-Mode US and HFR CEUS examinations. Participants were observed for 1 h after the puncture and were allowed to leave if no significant discomfort was noted.

Image interpretation and analysis

The US, HFR CEUS, and CVI-processed images were all independently reviewed by two individual radiologists with 10 years of experience in contrast US. Any discrepancies were resolved by consensus between the two. They were unaware of the histopathological results. LN CEUS characteristics were classified based on previous studies [13, 14] into the following patterns: (a) centrifugal enhancement (i.e., contrast bubble perfusion from the center to the periphery); (b) centripetal enhancement (i.e., contrast bubble perfusion from the periphery to the center); and (c) hybrid enhancement (i.e., no obvious directionality, with contrast bubble perfusion occurring simultaneously in the periphery and the center). In addition to these patterns, the presence or absence of perfusion defects served as a reference in order to distinguish the benign and malignant nature of LNs. The CVI assessment method was also based on the location and timing of contrast bubble appearance. The enhancement pattern of the lesioned LNs was similarly defined as (a) centrifugal enhancement (i.e., contrast bubbles were first tracked and color-coded in the center and then appeared in the distal end); (b) centripetal enhancement (i.e., contrast bubbles were first tracked and color-coded in the periphery and then appeared in the center); and (c) hybrid enhancement (i.e., contrast bubbles were tracked and color-coded simultaneously in the periphery and the center). Velocity variance of bubble flow was calculated as standard deviation (SD) of velocity of different bubbles throughout the same route and displayed as color maps from blue (low variance < 5 SD) to orange (high variance > 30 SD). Color maps were interpreted from blue to green (0–15 SD) as low-velocity variance and blue to orange (0–30 SD) as high-velocity variance for analysis. A sampling frame was used to sample the velocity within the lesioned LN in order to obtain velocity values for different sampling frames and to calculate their average.

Statistical analysis

Statistical analyses were performed using SPSS software 27.0 (IBM). Quantitative data were represented as means ± SDs and t tests were used for comparisons. Routine US and contrast parameters were compared using the chi-square test. Sensitivity, specificity, positive predictive value, and negative predictive value were compared using the McNemar test. The kappa test was utilized to compare the consistency of the two methods with pathological results, where $P < 0.05$ indicated a statistically significant difference.

Results

Participant characteristics

Of 44 patients screened for inclusion, 38 (mean age, 56 ± 16 years; 17 men and 21 women) with 42 LNs were included (Fig. 1). The 42 LN lesions were categorized based on their histological types. There were 24 malignant LNs, including metastatic squamous cell carcinoma ($n = 11$), lymphoma ($n = 7$), metastatic adenocarcinoma ($n = 1$), metastatic papillary thyroid carcinoma ($n = 4$), and metastatic neuroendocrine small cell carcinoma ($n = 1$). Benign histological presentations accounted for 18 LNs, including chronic inflammation ($n = 3$), lymphocytes ($n = 10$), and reactive hyperplasia ($n = 5$). Demographic and clinical pathological data for the LNs are presented in Table 1. There were differences in age and the VI in SMI and power Doppler results between benign and malignant LN lesions (P values, 0.004, 0.001, and 0.001, respectively). There were no differences in patient gender and maximum LN diameter (P values, 0.65 and 0.06, respectively).

HFR CEUS alone and HFR CEUS combined with CVI examination

The overall performance of HFR CEUS examination alone showed that 19 LNs were diagnosed as benign LNs, with 15 LNs confirmed by pathology, while 23 LNs were diagnosed as malignant LNs, with 20 ultimately confirmed by pathology. The sensitivity, specificity, positive predictive value, and negative predictive value of HFR CEUS examination alone were 83% (20 of 24 LNs; 95% confidence interval (CI): 62, 95), 83% (15 of 18 LNs; 95% CI: 58, 96), 87% (20 of 23 LNs; 95% CI: 65, 97), and 79% (15 of 19 LNs; 95% CI: 54, 93), respectively. The kappa value of 0.66 indicated a good agreement with pathological results.

The overall performance of the combination of HFR CEUS with CVI examination was as follows: 18 LNs were diagnosed as benign LNs, with 16 LNs confirmed by

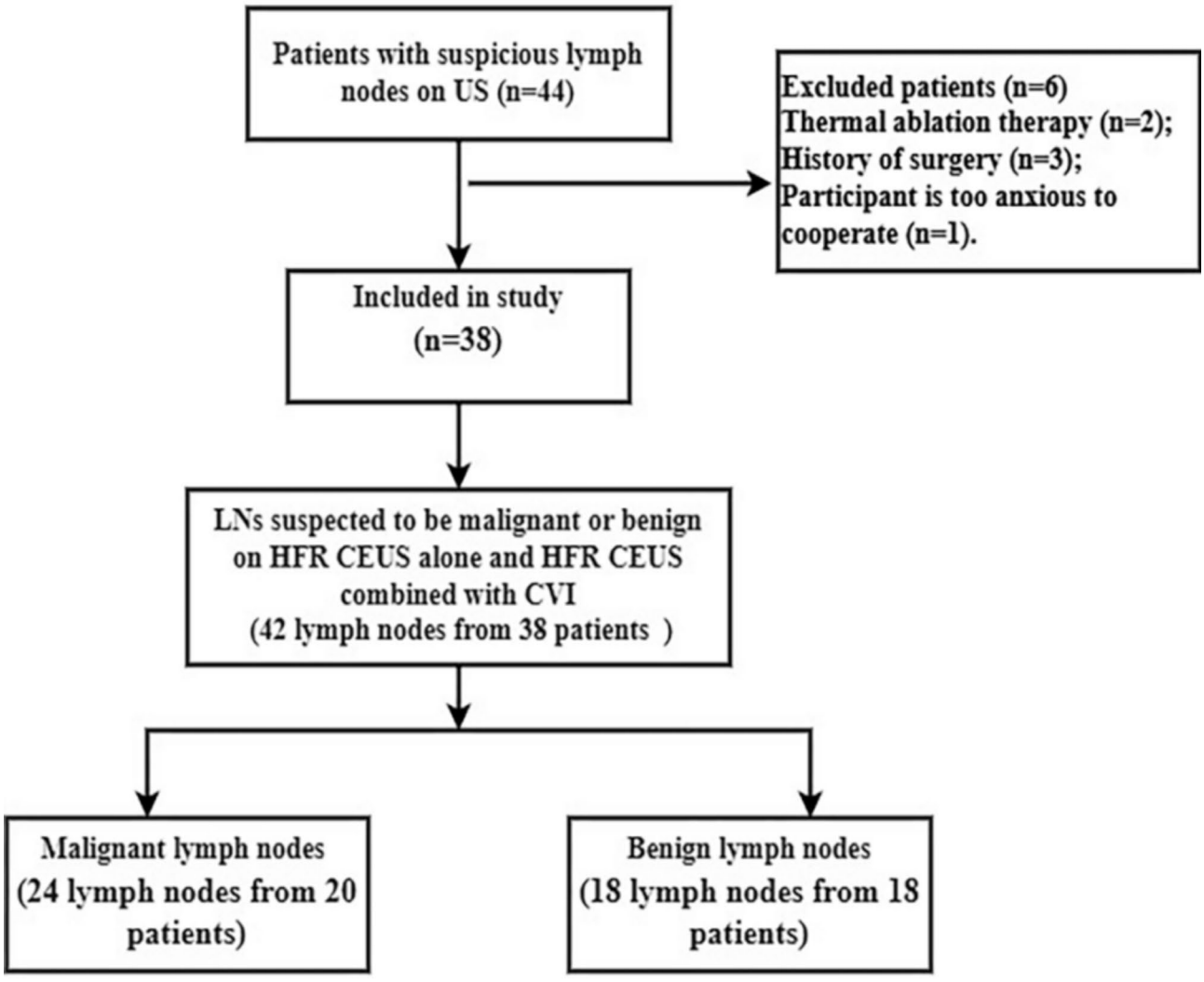

Fig. 1 Flowchart of participant selection. LN = lymph node, HFR CEUS = high-frame-rate contrast-enhanced ultrasound, HFR combined with CVI = high-frame-rate contrast-enhanced ultrasound combined with contrast vector imaging

Table 1 Basic characteristics of 42 lymph node lesions

Characteristic	Malignant	Benign	χ^2 or t text	*P*-Value
Age	66 ± 14	52 ± 15	−3.02	0.004
Sex*			0.20	0.65
M	10	7		
F	10	11		
Node lesions maximum diameter (mm)	14.47 ± 6.94	16.56 ± 6.14	−0.70	0.49
power Doppler flow index	31.87 ± 15.18	11.70 ± 8.70	−3.45	0.001
Microvascular flow index	43.74 ± 9.18	20.39 ± 11.79	−3.44	0.001

Note: HFR CEUS = High-frame-rate contrast-enhanced ultrasound, CVI = contrast vector imaging

*Data are numbers of participants

pathology, and 24 LNs were diagnosed as malignant LNs, with 22 LNs confirmed by pathology. The sensitivity, specificity, positive predictive value, and negative predictive value of HFR CEUS combined with CVI examination were 92% (22 of 24 LNs; 95% CI: 72, 99), 89% (16 of 18 LNs; 95% CI: 64, 98), 92% (22 of 24 LNs; 95% CI: 72, 99), and 89% (16 of 18 LNs; 95% CI: 64, 98), respectively. The kappa value of 0.81 indicated a very high agreement with pathological results. The combination of HFR CEUS with CVI examination improved the diagnostic accuracy for the benign and malignant nature of LNs. However, the

difference with HFR US contrast imaging alone was not statistically significant ($P = 0.33$).

In addition, only 11% of benign LNs (2 of 18) and 63% of malignant LNs (15 of 24) showed perfusion defects, and the difference between the two was statistically significant ($P < 0.001$).

In the HFR CEUS examination alone, 19 LNs exhibited a centrifugal enhancement pattern, 10 showed a centripetal enhancement pattern, and 13 displayed a hybrid enhancement pattern. HFR CEUS was combined with CVI examination, which modified the results of HFR CEUS examination alone. These outcomes included two LNs with a centrifugal pattern that were changed to a centripetal pattern, six LNs with a hybrid pattern that were modified to a centripetal pattern (Fig. 2), and one case with a hybrid pattern that was changed to a centrifugal pattern (Fig. 3). Pathological confirmation showed that the modified enhancement patterns were consistent with the pathological results, and the combined HFR CEUS with CVI examination increased the diagnostic value of contrast imaging for SLN lesions. The differences in enhancement patterns of benign and malignant SLNs in the contrast examination were statistically significant (all $P < 0.001$; Table 2).

Among the 42 LN lesions, there was no evidence of a difference between benign and malignant SLNs in terms of average velocity and velocity variance of CVI parameters. Benign LN velocity ranged from 4.6 mm/s to 31.7 mm/s, and malignant LN velocity ranged from 3.4 mm/s to 29.9 mm/s, ($P = 0.10$). Malignant LNs often demonstrated high velocity variance (21 out of 24), which was displayed as a variable color map from blue to orange. Some benign LNs also showed high velocity variance (13 out of 18), while the rest (5 out of 18) showed low velocity variance, displaying color images from blue to green ($P = 0.26$).

In malignant LNs, metastatic squamous cell carcinoma LNs were characterized by centripetal and hybrid

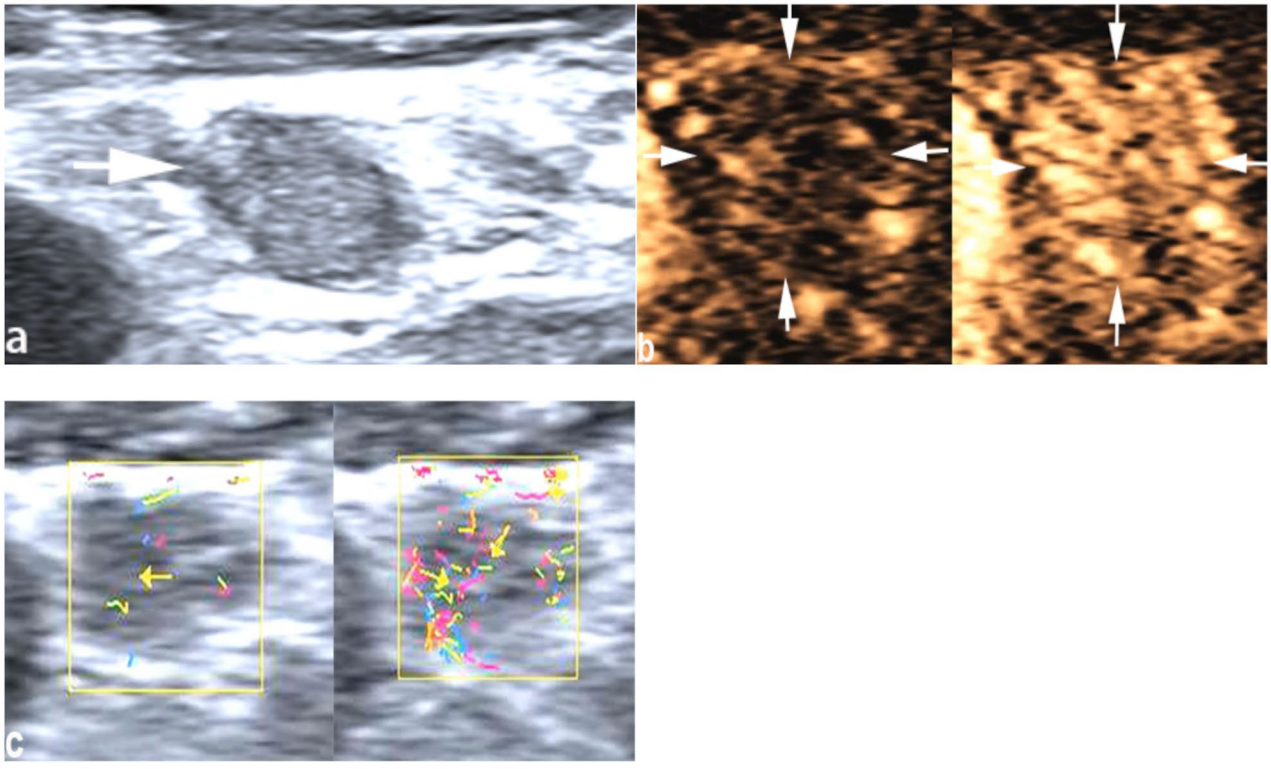

Fig. 2 Images in a 56-year-old female patient with papillary thyroid carcinoma with lymph node (LN) metastasis. **(a)** Conventional B-mode US shows an LN (5 × 3 mm) with a clear margin and regular shape and indistinct cortex-medulla boundary. **(b)** High-frame-rate contrast-enhanced ultrasound examination: The area indicated by the white arrow denotes the LN location. The left image shows the initial seconds (at 24–25 s) after the contrast agent enters the LN, with contrast bubbles visible both peripherally and centrally. The right image shows a few seconds later(at 25–27 s), with contrast bubbles rapidly filling the LN, presenting a mixed contrast pattern for the entire LN. **(c)** High-frame-rate contrast-enhanced ultrasound combined with contrast vector imaging (CVI) examination: The colored arrows within the yellow box represent the direction and trajectory of the movement of bubbles automatically tracked by CVI technology. The contrast bubble signal is captured by CVI technology and displayed with arrows indicating direction. The left image shows the initial seconds (at 24–25 s) after contrast injection, with contrast bubbles appearing mainly peripherally and arrows pointing toward the center. The right image shows a few seconds later(at 25–27 s), where contrast bubbles are moving from the periphery towards the center, with arrows pointing towards the center and displaying a centripetal contrast pattern. Pathological examination confirmed metastatic LN

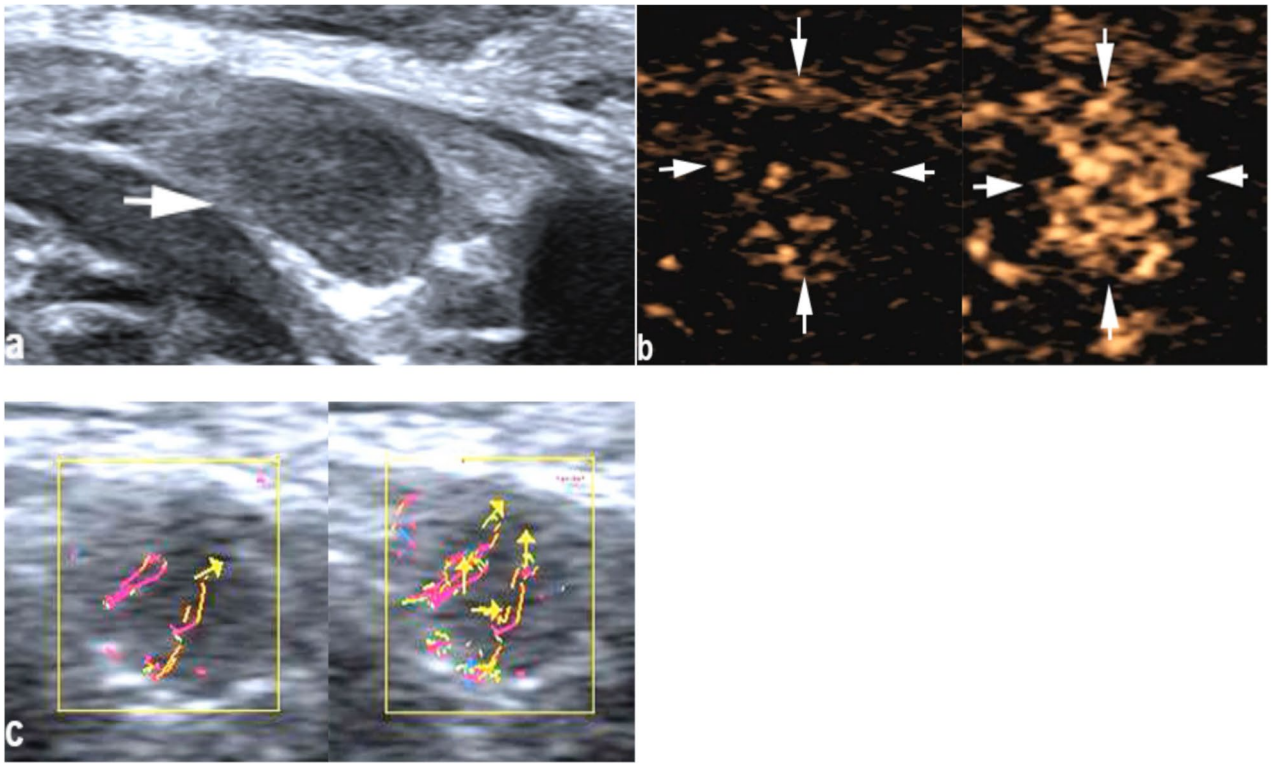

Fig. 3 Images in a 56-year-old female patient with a benign lymph node (LN). **(a)** Conventional B-mode US shows an LN (8×5 mm) with a clear margin and regular shape and indistinct cortex-medulla boundary. **(b)** High-frame-rate contrast-enhanced ultrasound examination: The area indicated by the white arrow denotes the LN location. The left image shows the initial seconds (at 9–10 s) after the contrast agent enters the LN, with contrast bubbles visible both peripherally and centrally. The right image shows a few seconds later (at10-11 s), with contrast bubbles rapidly filling the LN, presenting a mixed contrast pattern for the entire LN. **(c)** High-frame-rate contrast-enhanced ultrasound combined with contrast vector imaging (CVI) examination: The colored arrows within the yellow box represent the direction and trajectory of the movement of bubbles automatically tracked by CVI technology. The left image shows the initial seconds (at 9–10 s) after contrast injection, with contrast bubbles concentrated on one side and arrows indicating microbubble movement towards the periphery. The right image shows a few seconds later (at10-11 s), with a large number of contrast bubbles moving from the center to the periphery, arrows pointing towards the periphery and showing a lymphatic gate-like change and presenting a centrifugal contrast pattern. Pathological examination revealed inflammatory changes in the LN

Table 2 Comparison of benign and malignant lymph node enhancement patterns

Pathology results	HFR CEUS alone			HFR CEUS combined with CVI examination		
	Centripetal enhancement	Centrifugal enhancement	Hybrid enhancement	Centripetal enhancement	Centrifugal enhancement	Hybrid enhancement
Benign (18)	2	15	1	2	16	0
Malignant (24)	8	4	12	16	2	6
P-Value	< 0.001			< 0.001		

Note:HFR CEUS = High-frame-rate contrast-enhanced ultrasound, CVI = contrast vector imaging

enhancement patterns, while lymphoma-affected LNs had primarily hybrid enhancement patterns (Fig. 4). Benign LNs were characterized by a centrifugal enhancement pattern. The specific enhancement pattern characteristics of other pathological tissue types could not be summarized due to the small sample size. However, in general, malignant LN lesions were characterized by centripetal and hybrid enhancement patterns. Except for lymphoma LNs, other malignant LNs were more likely to exhibit perfusion defects, while benign LNs demonstrated a centrifugal enhancement pattern and were less likely to exhibit perfusion defects.

Discussion

SLN lesions are complex and diverse and accurately diagnosing their disease types is a significant challenge [15]. Therefore, identifying the benign or malignant lesion nature is crucial for patient treatment and prognosis. CVI technology has shown good feasibility in liver nodular lesion imaging in previous studies, the study has demonstrated that non-hepatocellular carcinoma tumors often

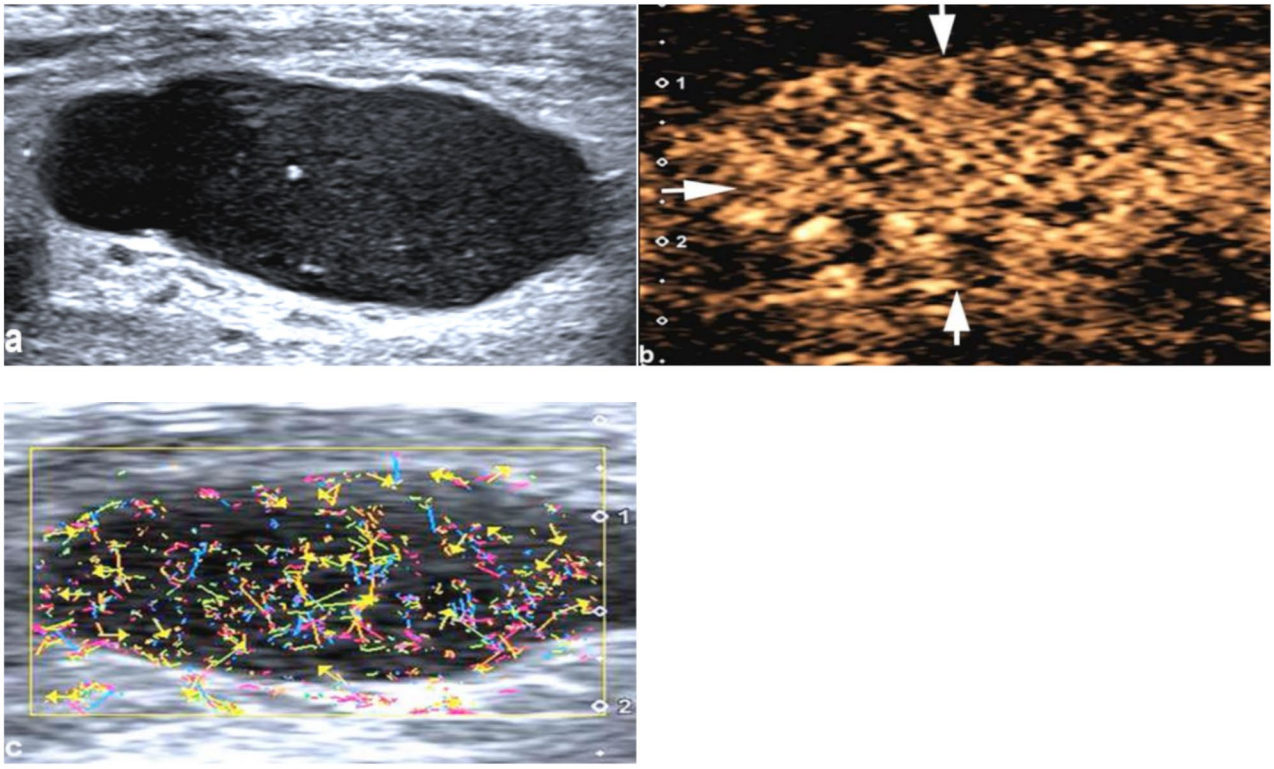

Fig. 4 Images in a 83-year-old male patient with cervical lymph node (LN) lymphoma. **(a)** Conventional B-mode US shows an LN (28 × 11 mm) with a punctate hyperechoic focus indicated by the white arrow. **(b)** High-frame-rate contrast-enhanced ultrasound: The area indicated by the white arrow denotes the LN location. The image shows contrast bubbles rapidly filling the LN from the center to the periphery, presenting a rapid mixed contrast pattern, also known as the "blizzard" pattern, where contrast bubbles quickly enter the LN from all directions, resembling a snowstorm. **(c)** High-frame-rate contrast-enhanced ultrasound combined with contrast vector imaging (CVI) examination: The colored arrows within the yellow box represent the direction and trajectory of the movement of bubbles automatically tracked by CVI technology. The image indicates the initial seconds after contrast injection, with contrast bubbles appearing both peripherally and centrally and disordered arrow directions. Pathological diagnosis identified lymphoma of the LN

display a peripheral rim-enhancing pattern with variable velocity, either high or low, whereas hepatocellular carcinoma typically presents with a staining pattern featuring feeding arteries and high-velocity variance on CVI [12], but it has not been applied in the field of SLN lesions. Therefore, the present study explored the diagnostic value and feasibility of post-processing CVI in assessing the benign and malignant nature of SLN lesions, focusing on the comparison of metastatic malignant LNs, lymphoma LN lesions, inflammatory reactive LNs, and reactive hyperplastic LNs. According to our preliminary evidence, HFR CEUS combined with CVI examination showed additional advantages over HFR CEUS alone because it can track and display color-coded movement of bubbles, increasing the visualization of the contrast pattern of the lesion LNs, which helps radiologists to analyze and interpret the contrast images and improves the diagnostic value of benign and malignant LN lesions.

In the present study, both HFR CEUS alone and HFR CEUS combined with CVI examination showed that the contrast pattern was centrifugal in benign LNs, including those with reactive hyperplasia and inflammatory reactive LNs. Only 11% of benign LNs had perfusion defects, while malignant LNs generally showed centripetal and hybrid contrast patterns and 63% demonstrated perfusion defects, This is consistent with previous studies. Prior studies have demonstrated that benign lymph nodes typically exhibit hilar blood flow patterns, whereas malignant lymph nodes tend to display peripheral or mixed patterns [11, 16]. It is possible that these specific enhancement patterns between malignant and benign LNs may be related to their blood supply methods.

Benign LNs usually have normal intact lymphatic gate structures, and their blood supply is provided from the central vessel to the lower branch vessels, thus showing centrifugal contrast pattern changes [16].

The LN is a lymphoid organ with a complex architecture organized into three approximately radial zones: cortex, paracortex, and medulla. In lymphatic fluid circulation, lymph fluid arrives at the outermost part of the organ, the capsule. Then, lymph fluid flows from the subcapsular sinus into the trabeculae and cortical sinuses and eventually through the medullary sinuses before leaving the LN through the efferent lymphatic vessel [17].

In metastatic LNs, tumor cells secrete soluble factors and extracellular vesicles during the lymphatic circulation process. These vesicles can locally affect the microenvironment of the LNs. Lymphatic endothelial cells exposed to tumor-derived small extracellular vesicles actively proliferate and reactivate their lymphangiogenic program characterized by sprouting, branching, and eventually forming a new vessel, which alters the normal blood supply of the LNs [18]. Thus, the outermost layer of metastatic LNs is first affected by tumor cells via lymphatic fluid circulation, leading to the formation of new blood vessels followed by an inward invasion, causing the affected LNs to exhibit a centripetal perfusion pattern [19]. Immature new blood vessels and avascular necrotic areas are common in cancerous metastatic LNs due to the fast tumor growth rate, which hinders the distribution of contrast agents to these areas, leading to perfusion defects.

The enhancement pattern of malignant lymphoma LNs is related to its pathological characteristics. Generally, lymphoma LNs have intact lymphatic gate structures, and tumor cells rarely accumulate under the capsule. Moreover, the blood vessels are highly proliferative and accompanied by small arterial dilation, making it easy for the contrast agent bubbles to flow and quickly distribute to the entire lymphoma. This manifests as a hybrid enhancement pattern. Thus, perfusion defects are less likely to occur compared to those in metastatic LNs. This observation is consistent with previous research [7, 20].

In the present study, the comparison of HFR CEUS alone and HFR CEUS combined with CVI examinations did not show statistically significant differences, which indicated that HFR CEUS examination is an advanced technique with a high value for SLN lesion diagnosis. However, the contrast patterns of lesion LNs that were small in volume and showed rapid arterial phase perfusion that could not be discerned by the naked eye were correctly modified with the assistance of CVI post-processing technology in the present study. As a result, two LNs with centrifugal patterns were changed to centripetal contrast pattern LNs, six LNs with hybrid contrast patterns were changed to centripetal contrast pattern LNs, and one case of hybrid contrast pattern was changed to centrifugal contrast pattern. The modified results were consistent with the pathological results, which reflects the value of CVI technology. As a technical supplement, CVI can help radiologists make more accurate visual diagnoses and improve the consistency between contrast and pathological results.

In the present study, SMI and power Doppler imaging technology were also included to assess the blood flow of LNs in conventional US. The study showed that malignant LNs have richer blood flow than benign LNs, which is consistent with previous research results [21, 22].

In summary, radiologists should consider various aspects of LN lesions and review multiple examination results, which is helpful for the diagnosis of SLN lesions. At the same time, HFR CEUS combined with CVI examination can effectively distinguish the benign and malignant nature of SLN lesions, which can make up for the shortcomings of ordinary US contrast examination and help radiologists to accurately analyze LN lesions.

There were some limitations in the study. First, the sample size was small. Second, due to the diversity of LN diseases, this study could only differentiate the benign and malignant LN lesions and could not provide accurate histopathological classification.A multi-center study with a larger sample size is required to further validate these findings.

In addition, a large-sample analysis of a specific superficial LN disease may yield surprising research results.

Supplementary Information

The online version contains supplementary material available at https://doi.org/10.1186/s12885-025-14190-0.

Supplementary Material 1

Supplementary Material 2

Supplementary Material 3

Supplementary Material 4

Author contributions

L.R. and L.X. collected and analyzed the data collection, and was a major contributor in writing the manuscript. W.J., H.R. and G.J. collected and organized the data. X.X. supervised the study and revised the manuscript. All authors read and approved the final manuscript.

Data availability

Data is provided within the manuscript.

Ethics declarations

Ethics approval and consent to participate

This study was approved by the medical ethics committee of the Second Affiliated Hospital of Anhui Medical University (approval number: YX2023-211). This study was performed in accordance with the Declaration of Helsinki. Written informed consent was obtained from all patients enrolled in this study.

Consent for publication

Not applicable.

Competing interests

The authors declare no competing interests.

Conflict of interest

The authors declare no competing interests.

Fund

No fund.

Received: 8 January 2025 / Accepted: 21 April 2025
Published online: 27 April 2025

References

1. Spiesecke P, Neumann K, Wakonig K, Lerchbaumer MH. Contrast-enhanced ultrasound (CEUS) in characterization of inconclusive cervical lymph nodes: a meta-analysis and systematic review. Sci Rep. 2022;12(1):7804.
2. Reticker-Flynn NE, Engleman EG. Lymph nodes: at the intersection of cancer treatment and progression. Trends Cell Biol. 2023;33(12):1021–34.
3. Moon IS, Kim DW, Baek HJ. Ultrasound-based diagnosis for the cervical lymph nodes in a tuberculosis-endemic area. Laryngoscope. 2015;125(5):1113–7.
4. Ahuja AT, Ying M. Evaluation of cervical lymph node vascularity: a comparison of colour doppler, power doppler and 3-D power doppler sonography. Ultrasound Med Biol. 2004;30(12):1557–64.
5. Rubaltelli L, Khadivi Y, Tregnaghi A, Stramare R, Ferro F, Borsato S, et al. Evaluation of lymph node perfusion using continuous mode harmonic ultrasonography with a second-generation contrast agent. J Ultrasound Med. 2004;23(6):829–36.
6. Esen G. Ultrasound of superficial lymph nodes. Eur J Radiol. 2006;58(3):345–59.
7. Dudau C, Hameed S, Gibson D, Muthu S, Sandison A, Eckersley RJ, et al. Can contrast-enhanced ultrasound distinguish malignant from reactive lymph nodes in patients with head and neck cancers? Ultrasound Med Biol. 2014;40(4):747–54.
8. Fei X, Han P, Jiang B, Zhu L, Tian W, Sang M, et al. High frame rate Contrast-enhanced ultrasound helps differentiate malignant and benign focal liver lesions. J Clin Transl Hepatol. 2022;10(1):26–33.
9. Giangregorio F, Garolfi M, Mosconi E, Ricevuti L, Debellis MG, Mendozza M, et al. High frame-rate contrast enhanced ultrasound (HIFR-CEUS) in the characterization of small hepatic lesions in cirrhotic patients. J Ultrasound. 2023;26(1):71–9.
10. Fei X, Li N, Zhu L, Han P, Jiang B, Tang W, et al. Value of high frame rate contrast-enhanced ultrasound in distinguishing gallbladder adenoma from cholesterol polyp lesion. Eur Radiol. 2021;31(9):6717–25.
11. Cai H, Liu S. The value of contrast-enhanced ultrasound versus shear wave elastography in differentiating benign and malignant superficial lymph node lesions. Am J Transl Res. 2021;13(10):11625–31.
12. Yoo J, Lee JM. Diagnostic value of high frame rate contrast-enhanced ultrasonography and Post-processing contrast vector imaging for evaluation of focal liver lesions: A feasibility study. Ultrasound Med Biol. 2020;46(9):2254–64.
13. Saito K, Okura H, Watanabe N, Hayashida A, Obase K, Imai K, et al. Comprehensive evaluation of left ventricular strain using speckle tracking echocardiography in normal adults: comparison of three-dimensional and two-dimensional approaches. J Am Soc Echocardiogr. 2009;22(9):1025–30.
14. Wang T, Xu M, Xu C, Wu Y, Dong X. Comparison of microvascular flow imaging and contrast-enhanced ultrasound for blood flow analysis of cervical lymph node lesions. Clin Hemorheol Microcirc. 2023;85(3):249–59.
15. Zhang Y, Luo Y, Zhang M, Yang M, Zhang Y, Li J, et al. Value of Contrast-enhanced ultrasound and conventional ultrasound in the diagnosis of papillary thyroid carcinoma with cervical lymph node metastases. Zhongguo Yi Xue Ke Xue Yuan Xue Bao. 2017;39(2):177–82.
16. Poanta L, Serban O, Pascu I, Pop S, Cosgarea M, Fodor D. The place of CEUS in distinguishing benign from malignant cervical lymph nodes: a prospective study. Med Ultrason. 2014;16(1):7–14.
17. Xin L, Yan Z, Zhang X, Zang Y, Ding Z, Xue H, et al. Parameters for Contrast-Enhanced ultrasound (CEUS) of enlarged superficial lymph nodes for the evaluation of therapeutic response in lymphoma: A preliminary study. Med Sci Monit. 2017;23:5430–8.
18. Gillot L, Baudin L, Rouaud L, Kridelka F, Noël A. The pre-metastatic niche in lymph nodes: formation and characteristics. Cell Mol Life Sci. 2021;78(16):5987–6002.
19. Tong J, Lin T, Wen B, Chen P, Wang Y, Yu Y et al. The value of multimodal ultrasound in diagnosis of cervical lymphadenopathy: can real-time elastography help identify benign and malignant lymph nodes? Front Oncol. 2023; 13(1073614.
20. García-Silva S, Peinado H. Mechanisms of lymph node metastasis: an extracellular vesicle perspective. Eur J Cell Biol. 2024;103(3):151447.
21. Aziz MU, Eisenbrey JR, Deganello A, Zahid M, Sharbidre K, Sidhu P, et al. Microvascular flow imaging: A State-of-the-Art review of clinical use and promise. Radiology. 2022;305(2):250–64.
22. Sim JK, Lee JY, Hong HS. Differentiation between malignant and benign lymph nodes: role of Superb microvascular imaging in the evaluation of cervical lymph nodes. J Ultrasound Med. 2019;38(11):3025–36.

Publisher's note